

5000

**Final Summary of Research Report  
October 1, 1998 – September 30, 2001**

**Planetary Geology and Geophysics Program  
“Dynamics and Structure of Planetary Rings”**

**Richard G. French, PI  
Astronomy Dept., Wellesley College  
Wellesley, MA 02481  
Grant Number NAG5-4046**

Our research funded under the PGG program during this period is summarized below. The publications resulting from this work are listed at the end of this document.

**1. Particle properties of Saturn’s rings**

We developed a novel technique to determine the macroscopic particle size distribution of the rings by exploiting diffraction effects during stellar occultations. This was a major undertaking, and resulted in two publications now in press (Nicholson *et al.* 2000, French and Nicholson 2000). In the latter paper, we derived power-law particle size distributions for each of Saturn’s main ring regions, using observations of the 3 July 1989 stellar occultation of 28 Sgr from Palomar, McDonald, and Lick Observatories. We used the Voyager PPS  $\delta$  Sco optical depth profile to estimate and then remove the directly transmitted signal from the 28 Sgr observations, leaving high SNR scattered light profiles at wavelengths of 3.9, 2.1, and 0.9  $\mu\text{m}$ . The angular distribution of this diffracted signal depends on the ring particle size distribution: the sharpness of the forward lobe is set by the largest particles, while the overall breadth and amplitude of the scattered signal reflects the abundance of smaller, cm-sized particles. We developed both a simple one-dimensional scattering model and a more realistic 2-D model. We assumed for simplicity a single power law particle size distribution for each major ring region, and determined the index  $q$  and lower and upper size cutoffs  $a_{\text{min}}$  and  $a_{\text{max}}$  that provide the best match to all three data sets in each region. Our results in the A and C Rings are fairly consistent with values of  $q$  and  $a_{\text{max}}$  derived from Voyager radio occultation (RSS) measurements (Zebker *et al.* 1985). We extended their results by determining *lower* limits to the particle size distributions and by probing the B Ring. This technique is applicable to imaging observations of the rings during the Cassini mission.

**2. Orbits of Saturn’s rings**

One of our ongoing projects is the continual improvement of the determination of Saturn’s pole direction and ring orbital elements. The predicted precession rate of Saturn’s spin vector, due principally to the indirect solar torque on Titan, is  $-0.783''/\text{yr}$ , corresponding to a period of 1.76 My (French *et al.* 1993). This result neglects the effects of Titan’s proper inclination of  $0.32^\circ$ , which leads to a slow variation in the torque exerted on Saturn with a period of  $\sim 700$  yr, Titan’s nodal regression period. At the present time, the torque is close to its minimum value, and our observed precession rate of  $-0.63'' \pm 0.23''$  (French *et al.* 1993), derived from Voyager and stellar occultation observations,

and  $=0.51''\pm 0.14''$  from a survey of 280 yr of historical data (Nicholson *et al.* 1999), is in excellent agreement with the nutation model of Vienne and Duriez (1992). As part of another joint effort, we collaborated with Amanda Bosh in her detailed analysis of Saturn's F ring (Bosh *et al.* 2000), recently submitted to *Icarus*.

### 3. Ring plane crossing observations

#### a) Small satellites and F ring clumps

Another major project, just completed, is our analysis of Hubble Space Telescope (HST) observations during the May, August and November 1995 Saturn's ring plane crossings (RPX). Our initial findings were presented in Nicholson *et al.* (1995). Our newest study, spearheaded by Co-Investigator Colleen McGhee, was published in *Icarus* (McGhee *et al.* 2000, attached). The edge-on geometry during the RPX allowed us to view Saturnian satellites normally hidden to Earth-based observers in the glare of the rings. We present new orbit solutions for many of Saturn's small satellites. While most satellites were found to be close to their expected positions based on previous orbital solutions (Nicholson *et al.* 1992, Jacobson 1996, and Harper and Taylor 1993), Prometheus lagged behind its predicted longitude by  $18.85^\circ\pm 0.04^\circ$ . A systematic drift in Pandora's longitude of  $-1.85^\circ$  relative to the Voyager ephemeris was observed between May and November. Refined methods of subtracting light from the edge-on rings led to additional detections of objects S/1995-S1 and S3 (Bosh and Rivkin 1995) in the May data, and S/1995-S5, S6, S7 (Nicholson *et al.* 1995) and S/1995-S9 (Roddier *et al.* 1995) in the August images. In addition to these previously-reported objects, eight new objects were identified during multiple HST visits in May and August; all have orbits consistent with that of the F ring and are likely to have been short-lived clumps within this ring, similar to those seen in Voyager images (Showalter 1997).

#### b) Photometry of the major satellites

We participated in the observations of Saturn's major satellites during the 1995 RPX campaign from Palomar, resulting in excellent photometric measurements of the inner Saturnian satellites (Buratti *et al.* 1998) over a large fraction of their full rotational light-curves. We find, for example, that Enceladus and Mimas are brighter on their trailing side, unlike Tethys, Rhea, and Dione, consistent with coating of these two satellites by material from the E ring.

### 4. Stellar occultations

We observed three stellar occultations by the Saturn system during the 1998 opposition, with the goals of obtaining stratospheric temperature profiles from the atmospheric events and constraints on Saturn's pole direction and ring geometry from ring event times. On 29 September, Saturn occulted GSC 0630-00405 (K=8.8), which we observed from the Calar Alto 3.5m telescope using the MAGIC infrared array camera at  $\lambda=2.2\ \mu\text{m}$ . We observed the 5 October occultation of GSC 0623-01090 (K=9.4) from three stations. At Calar Alto, observing conditions were quite good and we recorded the egress ring/atmosphere event at  $2.2\ \mu\text{m}$ . Egress was also observed from the Palomar 5m with an IR camera at  $\lambda=3.44\ \mu\text{m}$  to reduce the ring background to about 10 times the unocculted stellar flux. At ESO, the 3.6m telescope was equipped with the Adonis adaptive optics

system and the Sharp II IR camera in the K band. Ingress and egress ring and atmosphere events were observed under excellent conditions. Finally, the 14 Nov occultation of GSC 0622-00345 (K=8.4) was observed from the IRTF using NSFCAM. Analysis of these observations is nearly complete.

### 5. The Uranian rings

One of our most important long-term projects is the publication of our extensive set of Uranus ring observations, obtained under this program, and an associated comprehensive analysis of the orbits and structure of the rings. This is an iterative process, since refined orbital solutions for the rings affect the derived sky-plane and ring-plane event velocities, and thus the ring widths and optical depths (and also the event mid-times) derived from occultation profiles of the rings. Our most recent in-house orbital solution now includes all but two of our data sets (U138 and U144).

### 6. Giant planet atmospheres

Many of the observations obtained under this grant have involved occultations by planetary atmospheres, in addition to ring observations. Because it is most efficient to analyze the ring and atmospheric results at the same time, we have included as part of our PGG proposal each year the investigation the structure and dynamics of the stratospheres of the giant planets, as revealed by stellar occultations. [A small fraction of our total funding under this proposal has been provided by the Planetary Atmospheres program to support this work.] The principal derived quantity is the vertical temperature profile in the upper atmosphere, obtained by inversion of the atmospheric light curve. From the mean temperature, we learn about the diurnal and seasonal energetics of the atmosphere, and from the detailed structure in the vertical thermal profiles, we investigate, for example, the energetics of vertically-propagating inertia-gravity waves. **Figure 1** shows the temperature profile and vertical temperature gradient (lapse rate) of Saturn's stratosphere, obtained from our Palomar observations of a stellar occultation during the most recent RPX campaign (French *et al.* 1997).

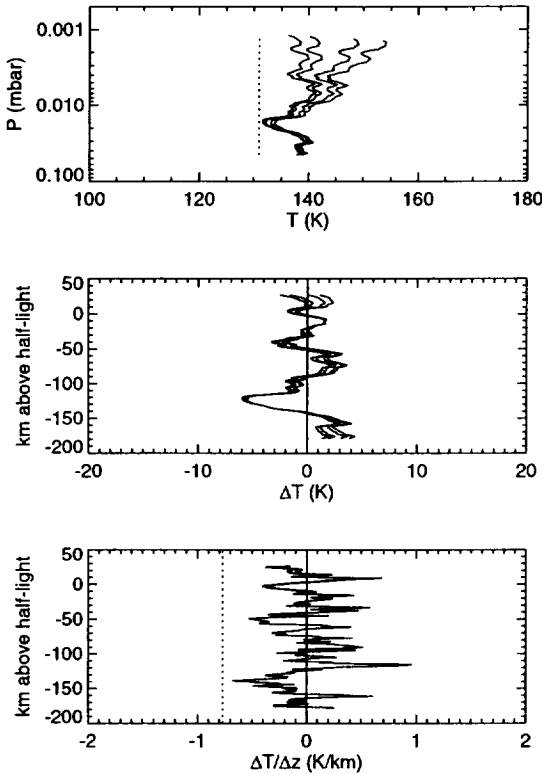


Figure 1 Saturn atmospheric structure